

## ULTRA-WIDEBAND SHORTED PATCH ANTENNAS FED BY FOLDED-PATCH WITH MULTI RESONANCES

H. Malekpoor\* and S. Jam

Department of Electrical and Electronic Engineering, Shiraz University of Technology, Shiraz 71555-313, Iran

**Abstract**—Novel designs of probe-fed broadband shorted patch antennas for ultra-wideband (UWB) applications are presented in this paper. In these designs, unequal resonance arms fed by a folded patch produce multi resonances to broaden the impedance bandwidth. In the first design, the antenna consists of an asymmetric E-shaped patch, a folded-patch feed and shorting pins. This antenna is achieved by four adjacent resonances with the measured  $-10$  dB impedance bandwidth of 76.18%. The pins are utilized to miniaturize the size of the patch. By introducing a folded ramp-shaped feed in the similar structure with the first design, a wider bandwidth with the five resonances is obtained. This improved design introduces an antenna with an impedance bandwidth of more than 110% and a considerable size reduction compared to the first antenna. The antennas present resonance tuning ability within the impedance bandwidth by varying the length of unequal arms. In addition, parametric studies are performed by investigating the effects of different key parameters on obtaining optimal designs of the proposed antennas.

### 1. INTRODUCTION

Microstrip patch antennas are rapidly developing in modern wireless communication systems, satellite and missile applications due to their appealing features, such as low profile, light weight and ease of fabrication. However, they have inherently narrow impedance bandwidth. There are various methods to overcome this serious drawback to achieve ultra-wideband (UWB) performance. Since the frequency range of the UWB wireless standard has been allocated from 3.1 to 10.6 GHz [1], nowadays obtaining a compact wideband antenna

---

*Received 16 August 2012, Accepted 24 September 2012, Scheduled 29 September 2012*

\* Corresponding author: Hossein Malekpoor (h.malekpoor@sutech.ac.ir).

is exclusively accentuated in commercial and military systems. Our proposed antennas operate in C-band, X-band and partially in S-band, which make those suitable for UWB applications such as Wireless Personal Area Network (WPAN), microwave imaging for detecting tumors and cancers, medical monitoring and home networking.

By reducing the size of microstrip antennas, the impedance bandwidth usually decreases. Hence, the problem of achieving the miniaturized antennas for broadband operation has been recently much regarded. Many techniques have been implemented in order to miniaturize the size of microstrip patch antennas such as utilizing a meandered patch or ground plane [2, 3] and using a shorting pin/wall [4–7]. By applying the shorting-pin loading technique a microstrip antenna treats as a quarter-wavelength structure. Several methods have been introduced to enhance the impedance bandwidth of microstrip antennas such as utilizing a thick substrate [8] and modification in the patch geometric structure like E-shaped patches [9–12], U-shaped-slot patches [13, 14] and V-shaped patch [15]. Other common methods to improve the impedance bandwidth are the implementation of stacked patch antennas [16, 17], L-probe feed [18, 19], shorted-patch [20, 21] and using shorting pins [22].

In previous works, an E-shaped patch antenna fed by a folded L-shaped probe with unequal arms provides an impedance bandwidth of 19.8% [23]. In [23], the asymmetric patch with dimensions of  $25 \times 27.7 \text{ mm}^2$ , which has been placed over the ground plane with dimensions of  $62.5 \times 100 \text{ mm}^2$ , produces three adjacent resonances to achieve a wideband antenna. Also, a microstrip antenna with unequal resonance arms of a modified E-shaped patch for producing different resonances has been exhibited in [24]. Recently, a new feeding method namely folded-patch feed, which can improve the impedance bandwidth of patch antenna, is proposed [25, 26]. An E-shaped patch antenna with a folded-patch feed technique is presented to have an impedance bandwidth of 73.78% [27]. Also, a polygonal-shaped patch antenna fed by a folded patch with shorting pins provides a large impedance bandwidth [28]. Moreover, a ramp fed patch antenna is introduced in [29]. In probe-fed UWB patch antennas, achieving the radiation patterns with acceptable stability and low cross-polarization level across the whole frequency range is quite a challenge [30]. Minimizing the variations of the gain and achieving a stable gain over the frequency band are also challenges in such structures.

In this article, probe-fed shorted patch antennas with an asymmetric rectangular patch based on unequal resonance arms and folded-patch feed's techniques to broaden the bandwidth are introduced. The first antenna is achieved by four resonances, which

includes impedance bandwidth ranging from 3.34 to 7.45 GHz. To cover completely UWB band (3.1–10.6 GHz) and achieving a wider bandwidth, the vertical folded-part of this antenna is ramped. In the improved design, by using a folded ramp-shaped feed, unequal arms and shorting pins five resonances are occurred to obtain an impedance bandwidth of more than 110%. Also, the physical dimension of this antenna is considerably reduced compared to the first antenna and importantly, it achieves a stable gain at about 6 dBi within a wide frequency range. The proposed antennas exhibit prominent features such as resonance tuning ability, comparatively simple structures and enhanced impedance bandwidth with stable radiation patterns across the entire operating bandwidth.

## 2. ANTENNAS DESIGN AND STRUCTURE

The coaxial probe feed is easy to fabricate with low spurious radiation related to other feeding methods. Hence, it is applied in the structures of the proposed antennas. It is well known that thick substrate and air dielectric constant substrate increase the bandwidth of the microstrip patch antennas. Generally, the microstrip antennas with probe feedings have lower impedance bandwidths due to their high Q factors. For a coaxially fed microstrip antenna, the substrate thickness is limited by the inductance of the feeding coaxial probe, which increases directly with increasing substrate thickness. To overcome this problem, the folded-patch feed technique with air substrate is introduced [25–28]. In this method, the low inductance contributed by the shorter coaxial probe is obtained.

The proposed antenna configurations are depicted in Figure 1. According to Figure 1(a), the first antenna is composed of an asymmetric E-shaped patch as upper patch, a folded-patch feed and shorting pins, which are placed over the ground plane with the size of  $60 \times 60 \text{ mm}^2$  and air substrate. The folded-patch feed with height  $h_1$  is applied to reduce the probe length and improve the impedance bandwidth. The asymmetric E-shaped patch with dimensions of  $34 \times 13 \text{ mm}^2$  is located at the height of  $h_2$  from the ground plane. As seen from Figure 1(b), the structure of the second antenna (improved antenna) is approximately similar to the first antenna, only with this difference that instead of the vertical folded-part, the folded ramp-shaped part is utilized. By introducing the proposed feeding technique, a new resonance at upper frequencies is obtained, thus the bandwidth is considerably widened. The dimensions of the asymmetric E-shaped patch for the second antenna are  $28 \times 10 \text{ mm}^2$  at the height  $h_4$  from the ground plane with the size of  $50 \times 50 \text{ mm}^2$ . It is obvious that the

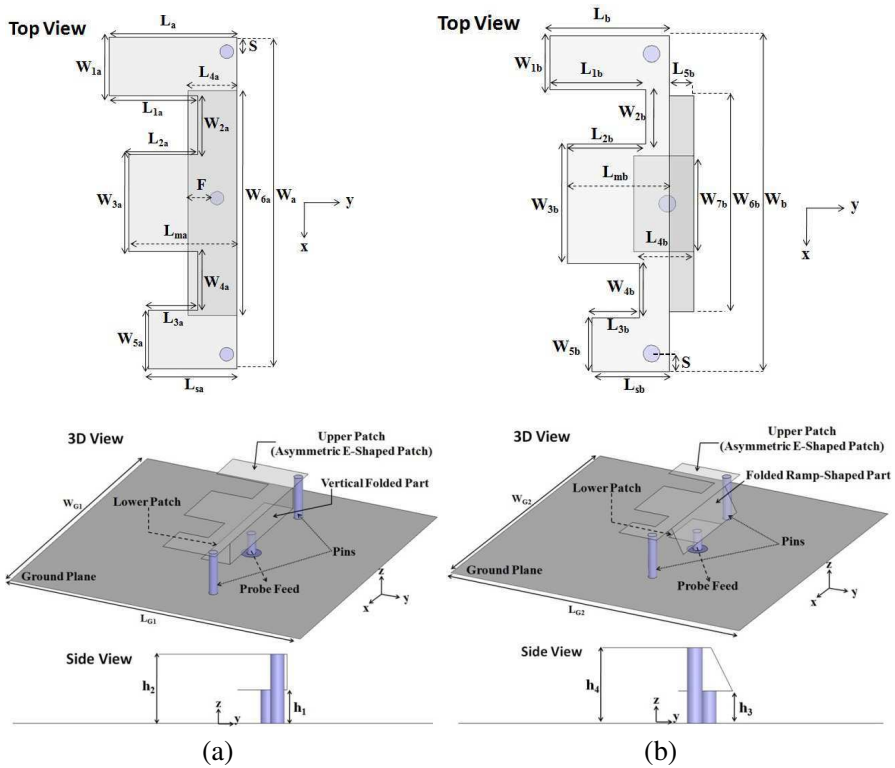


**Figure 1.** Geometry of the proposed antennas, (a) first antenna; (b) second antenna (improved antenna).

dimensions of the patch and ground plane at the second antenna is reduced with respect to the first antenna.

Two shorting pins, placed between the edge of the asymmetric E-shaped patch and the ground plane, present conventional  $\lambda/4$  shorted patches. Shorting pins with various diameters at different positions were investigated analytically to attain an optimal broadband performance. Those by producing one resonance at lower frequencies can be effected on achieving an acceptable miniaturization and a wider impedance bandwidth. According to the geometric structures of the proposed antennas in Figure 1, the optimized diameters of the pins are 1.4 mm.

The slot length, width and position on an E-shaped patch [9–11] play significant roles in achieving a wide bandwidth. Incorporating two parallel slots into the upper patch and unequal resonance arms, the asymmetric E-shaped patch produces three resonances. Therefore, a

wider impedance bandwidth can be achieved. An important advantage of the proposed antennas is their ability in tuning the resonances. The variations of slots' length and arms' length affect tuning the resonances. The total heights ( $h_2, h_4$ ) of the proposed antennas are 7 mm and the lengths of the probes ( $h_1, h_3$ ) are 3.4 mm and 3 mm, respectively. The second antenna has a wider bandwidth as compared with the antennas reported in [26, 27].

The proposed antennas are fabricated with 0.2 mm-thick copper plate. These antennas can be made from a single piece of copper plate without the need of soldering the folded part to the upper patch. Also, other important advantage of these antennas is simpler and easier fabrication process compared to similar antennas such as U-shaped-slot and L-shaped-slit patch [25] with folded-patch feed technique. The overall dimensions, slots' and arms' length are determined with parametric studies to obtain optimum design values. In addition, to choose proper dimension for an optimal design the minimal variations of the gain within the impedance bandwidth is considered. Several key parameters that help to achieve an optimal design are described in Section 4. The dimensions of the proposed antennas are given in Table 1.

### 3. RESULTS AND DISCUSSIONS

The simulation results are implemented using Ansoft HFSS version 12 with the finite element method. In this section, the measured and simulated results are separately investigated for two proposed

**Table 1.** Dimensions of the proposed antennas (units in mm).

First Antenna		Second Antenna (Improved Antenna)					
Parameters	Values	Parameters	Values	Parameters	Values		
$W_a$	34	$L_{3a}$	5	$W_b$	28	$L_{2b}$	6.5
$W_{1a}$	6	$L_{4a}$	5	$W_{1b}$	4.5	$L_{3b}$	4
$W_{2a}$	6	$L_{sa}$	9	$W_{2b}$	4.5	$L_{4b}$	5
$W_{3a}$	10	$L_{ma}$	11	$W_{3b}$	10	$L_{5b}$	2
$W_{4a}$	6	$h_1$	3.4	$W_{4b}$	4.5	$L_{sb}$	6.5
$W_{5a}$	6	$h_2$	7	$W_{5b}$	4.5	$L_{mb}$	8.5
$W_{6a}$	23	$L_{G1}$	60	$W_{6b}$	18	$h_3$	3
$L_a$	13	$W_{G1}$	60	$W_{7b}$	8	$h_4$	7
$L_{1a}$	9	$F$	3	$L_b$	10	$L_{G2}$	50
$L_{2a}$	7	$S$	1.5	$L_{1b}$	8	$W_{G2}$	50

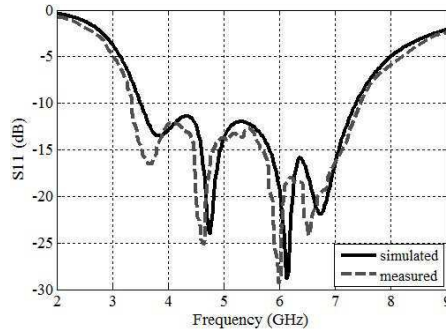


**Figure 2.** Reflection coefficients of the proposed first antenna.

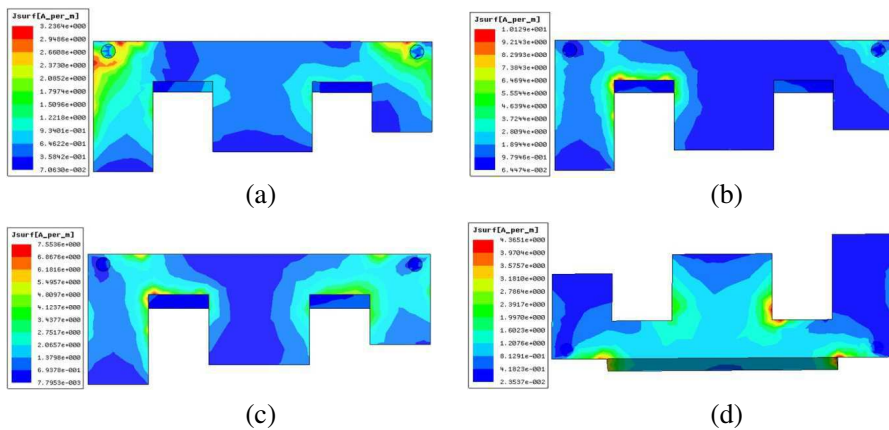
antennas. The measured results are in good agreement with simulation results obtained using a finite ground plane. Usually accomplished researches use only two/three adjacent resonances to make a patch antenna wideband [23] and [25–27]. In this study, four/five obvious adjacent resonances are observed in the obtained results of the proposed designs.

### 3.1. First Antenna

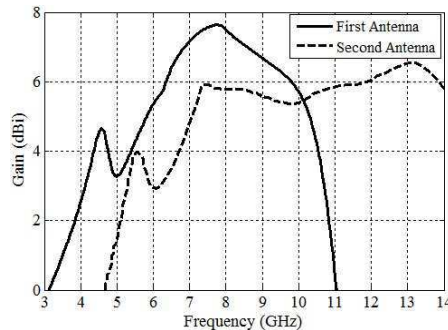
As shown in Figure 2, the proposed first antenna operates from 3.34 GHz to 7.45 GHz and its measured  $-10$  dB impedance bandwidth is 76.18%. The first antenna indicates an enhancement of more than 22% in impedance bandwidth compared to the antenna reported in [25]. Also, the impedance bandwidth of the proposed antenna is more than triple of that of the E-shaped patch antenna with unequal resonance arms in [23]. The width, length and total height of the patch in terms of wavelength at the lower end of the frequency band are  $0.379\lambda_{L1}$ ,  $0.145\lambda_{L1}$  and  $0.078\lambda_{L1}$ , respectively, whereas the length of probe is  $0.038\lambda_{L1}$ . Four resonant frequencies ( $f_{res1}$ ,  $f_{res2}$ ,  $f_{res3}$ , and  $f_{res4}$ ) of the first antenna are 3.82, 4.74, 6.13, and 6.73 GHz, respectively. Also, to highlight the performance of the first antenna, it is compared with the conventional E-shaped patch antenna reported in [9]. In [9], an impedance bandwidth of 32.3% in the frequency range 2.05–2.84 GHz is obtained with an antenna size of  $70 \times 45 \times 10$  mm<sup>3</sup>. Thus, our design results in 43.88% increase in frequency bandwidth and 36.93% size reduction.

Figure 3 depicts the surface current distribution on the patch at four frequencies. As seen from Figure 3(a), at the first resonance a  $\lambda/4$  current distribution dominates around pins. Thus, the first resonance is essentially determined by shorting pins. It is clear that at the

second resonance of 4.74 GHz, a typical  $\lambda/4$  patch antenna is exhibited. The non-uniform current distribution along  $y$ -axis is observed with concentration around the slot between the longer arm and the middle arm, as shown in Figure 3(b). This is due to the asymmetry of the antenna. Thus, it is concluded that the second resonance corresponds to the longer arm. The third resonance is at 6.13 GHz, where a  $\lambda/2$  resonant antenna is exhibited. The concentration of current is around the slots of the asymmetric E-shaped patch and on the edges of folded part, as shown Figure 3(c). Thus, we can say that the third resonance corresponds to the middle arm. Similarly, at the fourth resonance of 6.73 GHz, a  $\lambda/2$  resonant antenna is exhibited. As shown



**Figure 3.** Current distribution on the patch of the first antenna at different frequencies. (a)  $f_{res1} = 3.82$  GHz; (b)  $f_{res2} = 4.74$  GHz; (c)  $f_{res3} = 6.13$  GHz; (d)  $f_{res4} = 6.73$  GHz.



**Figure 4.** Gain of the proposed antennas.

in Figure 3(d), the current distribution concentrates on the overall of the folded part specifically on its edges and the area of the upper patch which connects to the folded part.

According to the gain of the proposed antennas in Figure 4, the maximum gain of the first antenna within the bandwidth is more than 7.5 dBi. It is clearly observed that with an increase in the frequency within operating band, the gain of antenna increases as well. The measured and simulated radiation patterns in the  $xz$ -plane ( $E$ -plane) and  $yz$ -plane ( $H$ -plane) are shown in Figure 5. It can be seen that there is a good agreement between the measured and simulated results. The measured and simulated radiation patterns in three frequencies across the whole operating bandwidth are stable. Also, the radiation patterns are not exactly symmetric for electric fields in both planes because of its asymmetric structure. Nevertheless, the antenna presents good broadside radiation patterns. Meanwhile, the cross-polarization level

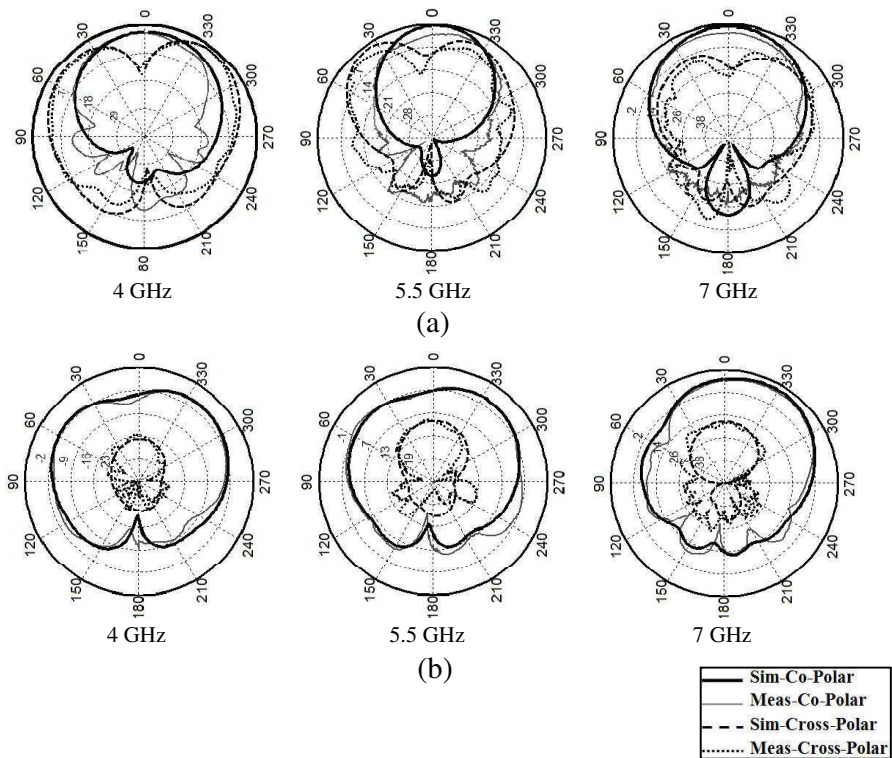


**Figure 5.** Measured and simulated radiation patterns of the first antenna. (a)  $xz$ -plane ( $E$ -plane); (b)  $yz$ -plane ( $H$ -plane).

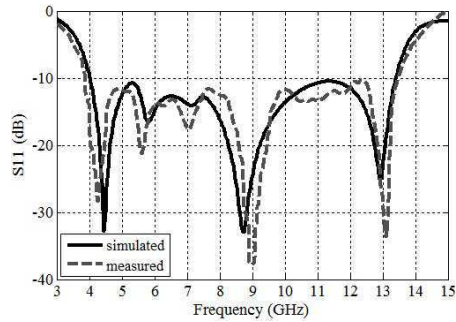


**Figure 6.** Reflection coefficients of the proposed second antenna.

in the  $E$ -plane is higher than that in the  $H$ -plane. This is mainly due to the feed location on  $y$ -axis and the discontinuity in the structure obtained using the shorting pins. The probe feed possesses inherent asymmetry which generates higher order modes and consequently produces cross-polarized radiation. Also, shorting pins by introducing the asymmetry of the structure can effect on the increase of the contribution of the cross-polarized radiation.

### 3.2. Second Antenna (Improved Antenna)

Figure 6 reveals that the proposed second antenna operates from 3.87 to 13.46 GHz with the measured impedance bandwidth of 110.7%. In comparison with the first antenna, it presents an enhancement of more than 34% in impedance bandwidth. The impedance bandwidth of the improved antenna is more than 90% than the E-shaped patch antenna with unequal arms in [23]. Also, the impedance bandwidth of this antenna is about 38% and 36% wider than the presented antennas in [26] and [27], respectively. The width, length and total height of patch of the second antenna in terms of wavelength at the lower end of the frequency band are  $0.361\lambda_{L2}$ ,  $0.129\lambda_{L2}$  and  $0.090\lambda_{L2}$ , respectively, whereas the length of probe is  $0.039\lambda_{L2}$ . It is clear that the improved antenna with a shorter probe length than the first antenna achieves a broader bandwidth. Five resonant frequencies ( $f_{r1}$ ,  $f_{r2}$ ,  $f_{r3}$ ,  $f_{r4}$ , and  $f_{r5}$ ) of the second antenna are 4.47, 5.78, 7.12, 8.70 and 12.93 GHz, respectively.

Figure 7 demonstrates the current distribution on the patch at five resonant frequencies. As seen from Figure 7(a), at the first resonance a  $\lambda/4$  current distribution dominates around pins that indicate the effect of pins on determining the first resonance. As shown in Figures 7(b), (c) and (d), the current distribution is similar to the first antenna. As

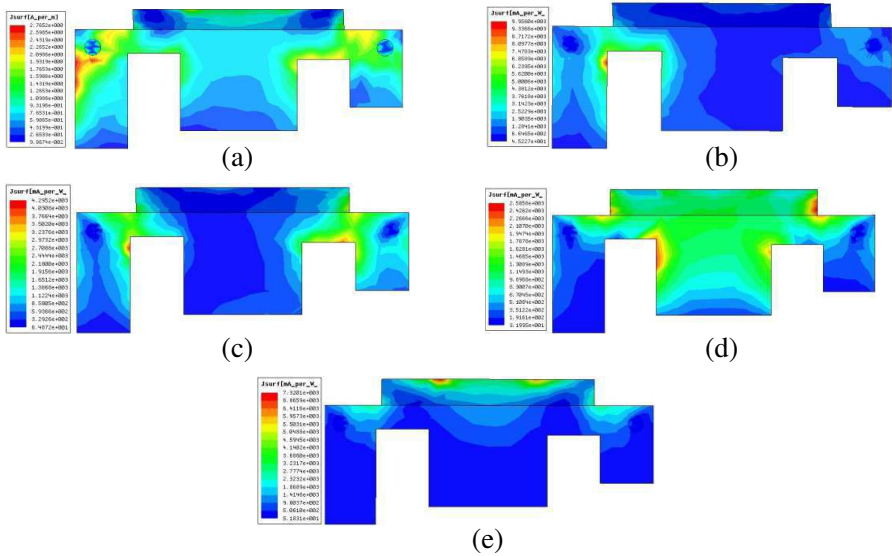


**Figure 7.** Current distribution on the patch of the second antenna at different frequencies. (a)  $f_{r1} = 4.47$  GHz; (b)  $f_{r2} = 5.78$  GHz; (c)  $f_{r3} = 7.12$  GHz; (d)  $f_{r4} = 8.70$  GHz; (e)  $f_{r5} = 12.93$  GHz.

explained about current distribution at the first antenna, the second and third resonances at the second antenna correspond to the longer and middle arms, respectively. As seen from Figure 7(e), at the fifth resonance the current concentrates on the edge of the folded ramp-shaped part which connects to the lower patch.

The gain of the second antenna is shown in Figure 4. It is observed that the improved antenna attains a stable gain at about 6 dBi within a wide frequency range from 7 to 12 GHz. The radiation patterns for frequencies 4.47, 8.70 and 12.93 GHz in the  $xz$ -plane ( $E$ -plane) and  $yz$ -plane ( $H$ -plane) are shown in Figure 8. Despite increasing the bandwidth, the broadside radiation patterns across the whole operating band remain stable.

#### 4. PARAMETRIC STUDY ON KEY PARAMETERS

In this section, to explicitly describe the mechanism of the performance of antennas, the effects of different key parameters are discussed. The parametric study include some of the important parameters for achieving the optimal designs, namely the probe length (height of the lower patch), shorting pins, length of the slots and arms, and width of

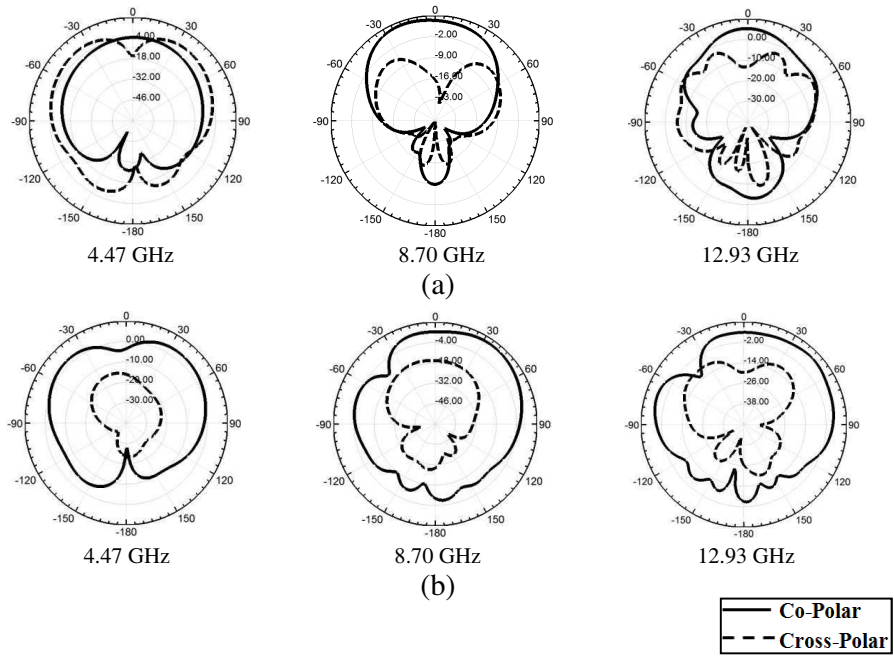


**Figure 8.** Radiation patterns of the second antenna. (a)  $xz$ -plane; (b)  $yz$ -plane.

the folded ramp-shaped part.

#### 4.1. The Probe Length (Height of the Lower Patch)

Figure 9 shows the variations of the probes length ( $h_1, h_3$ ). It clearly shows that as the lengths  $h_1$  and  $h_3$  increase, the probe feed's inductance increases, impedance matching deteriorates, and consequently the impedance bandwidth decreases. When the probe length reduces from an optimized value, the capacitive effects dominate, which results in worse impedance bandwidth. The optimum values of  $h_1$  and  $h_3$  for proposed antennas are 3.4 mm and 3 mm, respectively. Moreover, the optimized values of  $h_2$  and  $h_4$  are 7 mm for broadening the impedance bandwidth.

#### 4.2. Shorting Pins

Shorting pins make the antennas resonate at a much lower frequency compared with the antennas without shorting pins. Therefore, the antennas with an acceptable miniaturization can be achieved. The

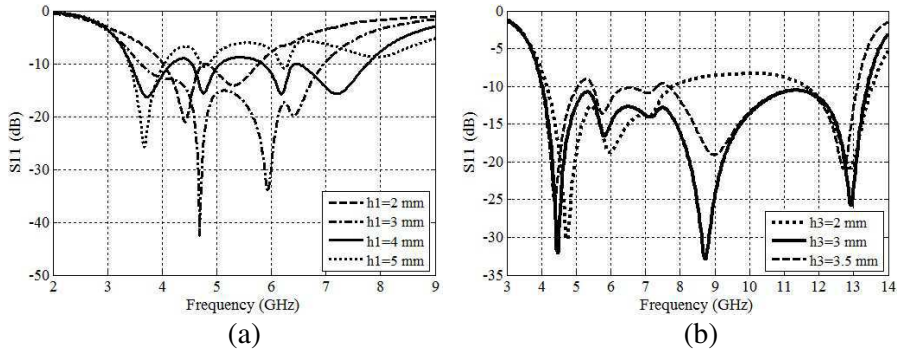


**Figure 9.** Simulated  $S_{11}$  for different lengths of coaxial probe feed, (a) first antenna; (b) second antenna.

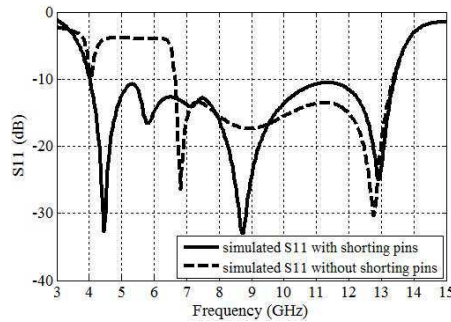


**Figure 10.** Simulated  $S_{11}$  of the second antenna with and without shorting pins.

effect of the shorting pins on the second antenna's performance is shown in Figure 10. The impedance bandwidth of the second antenna without shorting pins is 67.47% in the frequency range 6.64–13.40 GHz. Thus, the second antenna with shorting pins results in more than 43% increase in frequency bandwidth. The first resonance in both antennas is mainly excited by shorting pins, as shown in Figures 3(a) and 7(a).

### 4.3. Length of the Slots and Arms

Figure 11 demonstrates the variations of slots' and arms' length for the first antenna. The first resonance is mainly determined by length  $L_a$  of the upper patch, as shown in Figure 3(b). As seen from Figures 3(b) and (c), it is found that the length of slot  $L_{1a}$  affects the second and third resonances. Therefore, as shown Figure 11(a), with the increase

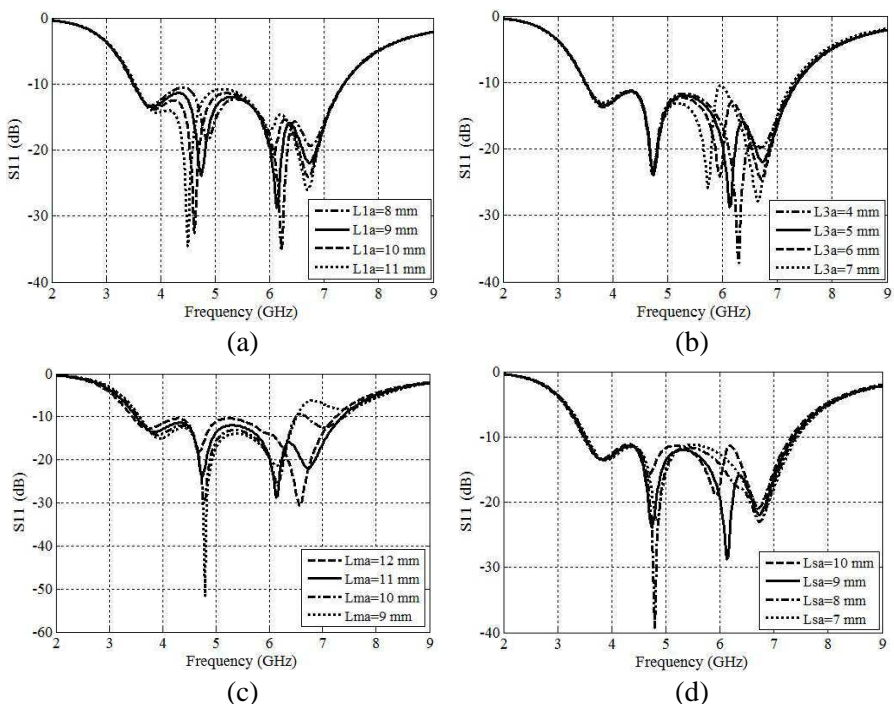


**Figure 11.** Reflection coefficients of the first antenna for different, (a) slot length  $L_{1a}$ ; (b) slot length  $L_{3a}$ ; (c) middle arm  $L_{ma}$ ; (d) shorter arm  $L_{sa}$ .

of  $L_{1a}$  the second and third resonances decrease and that is due to the fact that the current paths at these frequencies increase. Similarly, according to Figure 11(b), when the slot length  $L_{3a}$  increases, the third resonance drastically decreases, because the current paths increase. Furthermore, the variations of  $L_{3a}$  have a little effect on the fourth resonance, whereas the first and second resonances remain unchanged.

The third resonant frequency of first antenna is mainly determined by the length of middle arm,  $L_{ma}$ , of the upper patch. As shown in Figure 11(c), with an increase in  $L_{ma}$ , the second and fourth resonances decrease, because the current paths prolong at these frequencies. The variations of shorter arm  $L_{sa}$  of the upper patch are shown in Figure 11(d). With an increase in  $L_{sa}$ , as the current paths at these frequencies increase, the second and third resonances mainly decrease. However, the first and fourth resonances remain without change. Therefore, it is concluded that third resonance can be determined by  $L_{sa}$ . The optimum values for lengths of the middle and shorter arms are

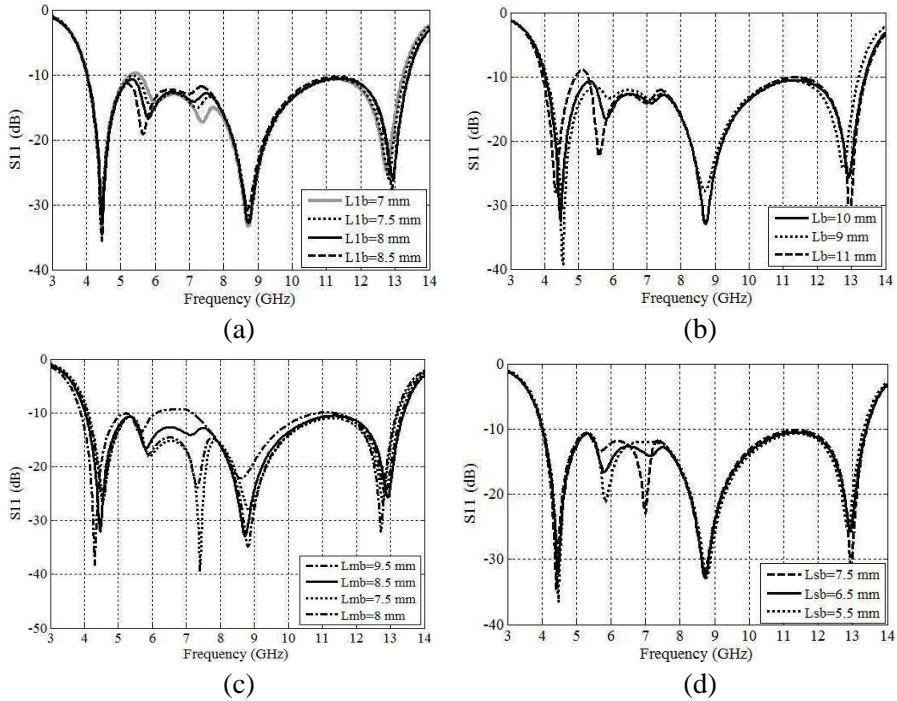


**Figure 12.** Reflection coefficients of the second antenna for different, (a) slot length  $L_{1b}$ ; (b) longer arm  $L_b$ ; (c) middle arm  $L_{mb}$ ; (d) shorter arm  $L_{sb}$ .

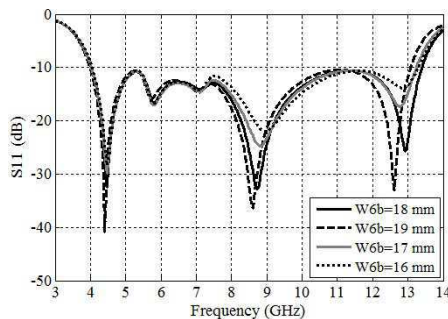
found 11 mm and 9 mm, respectively to achieve the optimal broadband performance.

Figure 12 depicts the variations of slots' and arms' length for the second antenna. Figure 12(a) demonstrates the variations of the slot's length  $L_{1b}$ . With an increase in  $L_{1b}$ , the second and third resonances explicitly reduce, whereas the first, fourth and fifth resonances are stationary. As can be seen from Figure 12(b), with the increase of the longer arm,  $L_b$  the second resonance drastically decreases and first resonance slightly also decreases, whereas other resonances stay fixed. Hence, the second resonance can be mainly excited by the longer arm. According to Figure 12(c), by increasing  $L_{mb}$ , the second and fourth resonances decrease. Thus, similar to the first antenna can be concluded that the middle arm is a major part in exciting the third resonance. It is clearly indicated in Figure 12(d) that with an increase in  $L_{sb}$ , the second and third resonances reduce. The fourth resonance remains unchanged and we can say that it is principally determined

by shorter arm. Optimum values of  $L_b = 10$  mm,  $L_{1b} = 8$  mm,  $L_{mb} = 8.5$  mm and  $L_{sb} = 6.5$  mm are chosen for the optimal second antenna design.

#### 4.4. Width of the Folded Ramp-shaped Part

Figure 13 shows the effect of width of the folded ramp-shaped part for the second antenna. The results show that the fifth resonance can be drastically shifted by adjusting  $W_{6b}$ . By increasing  $W_{6b}$ , the fifth resonance appears with better impedance matching until the width of folded ramp-shaped part possesses an optimum value for achieving the maximum of bandwidth. The first, second and third resonances are fixed. However, the fourth resonance shifts downward which it is confirmable by current distribution at this frequency, according to Figure 7(d). Therefore, it can be comprehended that a new resonance at the second antenna is principally determined by folded ramp-shaped part. Also, it should be mentioned that the optimized dimensions and positions of the folded ramp-shaped part and the lower patch are key parameters to achieve an excellent impedance bandwidth and exciting the fifth resonance. A value of 18 mm is found for  $W_{6b}$  to provide the optimal ultra-wideband operation. The photograph of the fabricated antennas is shown in Figure 14.



**Figure 13.** Reflection coefficients of the second antenna for different widths of the folded ramp-shaped part.



**Figure 14.** Fabrication of the proposed antennas.

## 5. CONCLUSION

With the implementation of shorted asymmetric E-shaped patches fed by folded patch, compact broadband antennas are achieved. The first antenna by producing the four resonances includes the impedance bandwidth from 3.34 to 7.45 GHz. By introducing the recommended feeding technique at the second antenna namely folded ramp-shaped feed, a new resonance with good impedance matching is occurred, thus the bandwidth is drastically enhanced. It has been formed by the five resonances with the similar structure to the first antenna for covering the frequency range 3.87–13.46 GHz. The main features of the presented antennas are their ability in tuning the resonances, acceptable miniaturization and enhanced bandwidth with comparatively simple structures. Low cross-polarization levels in the  $H$ -plane and stable radiation patterns in both planes are obtained. More importantly, the improved antenna achieves a stable gain at about 6 dBi within a wide frequency range. In addition, the performance of broadening the impedance bandwidth is explored by investigating the behavior of the surface currents on the patches.

## REFERENCES

1. Wei, L.-A., "Applications of ultra wideband," M.S., The University of Texas at Arlington, Dec. 2006.
2. Wong, K. L., C. L. Tang, and H. T. Chen, "A compact meandered circular microstrip antenna with a shorting pin," *Microw. Opt. Technol. Lett.*, Vol. 15, No. 3, 147–149, Jun. 1997.
3. Kuo, J. S. and K. L. Wong, "A compact microstrip antenna with meandering slots in the ground plane," *Microw. Opt. Technol. Lett.*, Vol. 29, 95–97, Apr. 20, 2001.
4. Waterhouse, R., "Small microstrip patch antenna," *Electron. Lett.*, Vol. 31, No. 8, 604–605, 1995.
5. Wang, Y. J., C. K. Lee, and W. J. Koh, "Single-patch and single-layer square microstrip antenna with 67.5% bandwidth," *IEE Proc. Microw. Antennas Propag.*, Vol. 148, 418–422, 2001.
6. Quenvedo-Teruel, Q., E. Pucci, and E. Rajo-Iglesias, "Compact loaded PIFA for multifrequency applications," *IEEE Trans. Antennas Propag.*, Vol. 58, No. 3, 656–664, Mar. 2010.
7. Sim, Z. W., R. Shuttleworth, M. J. Alexander, and B. D. Grieve, "Compact patch antenna design for outdoor RF energy harvesting in wireless sensor networks," *Progress In Electromagnetics Research*, Vol. 105, 273–294, 2010.

8. Schaubert, D. H., D. M. Pozar, and A. Adrian, "Effect of microstrip antenna substrate thickness and permittivity: Comparison of theories and experiment," *IEEE Trans. Antennas Propag.*, Vol. 37, 677–682, Jun. 1989.
9. Yang, F., X. X. Zhang, X. N. Ye, and Y. Rahmat-Samii, "Wideband E-shaped patch antennas for wireless communications," *IEEE Trans. Antennas Propag.*, Vol. 49, No. 7, 1094–1100, Jul. 2001.
10. Ge, Y., K. P. Esselle, and T. S. Bird, "E-shaped patch antennas for high-speed wireless networks," *IEEE Trans. Antennas Propag.*, Vol. 52, 3213–3219, 2004.
11. Ang, B. K. and B. K. Chung, "A wideband E-shaped microstrip patch antenna for 5–6 GHz wireless communications," *Progress In Electromagnetics Research*, Vol. 75, 397–407, 2007.
12. Islam, M. T., M. N. Shakib, and N. Misran, "Broadband E-H shaped microstrip patch antenna for wireless systems," *Progress In Electromagnetics Research*, Vol. 98, 163–173, 2009.
13. Khodaei, G. F., J. Nourinia, and C. Ghobadi, "A practical miniaturized U-slot patch antenna with enhanced bandwidth," *Progress In Electromagnetics Research B*, Vol. 3, 47–62, 2008.
14. Vedaprabhu, B. and K. J. Vinoy, "An integrated wideband multifunctional antenna using a microstrip patch with two U-slots," *Progress In Electromagnetics Research B*, Vol. 22, 221–235, 2010.
15. Elsadek, H. and D. M. Nashaat, "Multiband and UWB V-shaped antenna configuration for wireless communications applications," *IEEE Antennas Wireless Propag. Lett.*, Vol. 7, 89–91, 2008.
16. Matin, M. A., B. S. Sharif, and C. C. Tsimenidis, "Probe fed stacked patch antenna for wideband applications," *IEEE Trans. Antennas Propag.*, Vol. 55, No. 8, 2385–2388, Aug. 2007.
17. Ooi, B. L., S. Qin, and M. S. Leong, "Novel design of broadband stacked patch antenna," *IEEE Trans. Antennas Propag.*, Vol. 50, No. 8, 1391–1395, 2002.
18. Guo, Y. X., C. L. Mak, K. M. Luk, and K. F. Lee, "Analysis and design of L-probe proximity fed-patch antennas," *IEEE Trans. Antennas Propag.*, Vol. 49, 145–149, 2001.
19. Islam, M. T., M. N. Shakib, and N. Misran, "Design analysis of high gain wideband L-probe fed microstrip patch antenna," *Progress In Electromagnetics Research*, Vol. 95, 397–407, 2009.
20. Kuo, J. S. and K. L. Wong, "A low-cost microstrip-line-fed shorted-patch antenna for a PCS base station," *Microw. Opt.*

- Technol. Lett.*, Vol. 29, No. 3, 146–147, 2001.
21. Lau, K. L., S. H. Wong, and K. M. Luk, “Wideband folded shorted patch antenna with double L-slots,” *Electron. Lett.*, Vol. 43, 515–517, Nov. 2007.
  22. Guha, D. and Y. M. M. Antar, “Circular microstrip patch loaded with balanced shorting pins for improved bandwidth,” *IEEE Antennas Wireless Propag. Lett.*, Vol. 5, 217–219, Dec. 2006.
  23. Xiong, J., Z. Ying, and S. He, “A broadband low profile patch antenna of compact size with three resonances,” *IEEE Trans. Antennas Propag.*, Vol. 57, 1838–1843, 2009.
  24. Peng, L., C. L. Ruan, and X. H. Wu, “Design and operation of dual/triple-band asymmetric M-shaped microstrip patch antennas,” *IEEE Antennas Wireless Propag. Lett.*, Vol. 9, 1069–1072, 2010.
  25. Chiu, C. Y., K. M. Shum, C. H. Chan, and K. M. Luk, “Bandwidth enhancement technique for quarter-wave patch antennas,” *IEEE Antennas Wireless Propag. Lett.*, Vol. 2, 130–132, Dec. 2003.
  26. Chiu, C. Y., C. H. Chan, and K. M. Luk, “Study of small wideband patch antenna with double shorting walls,” *IEEE Antennas Wireless Propag. Lett.*, Vol. 3, 230–231, Dec. 2004.
  27. Chiu, C. Y., H. Wong, and C. H. Chan, “Study of small wideband folded-patch-feed antennas,” *IET Microw. Antennas Propag.*, Vol. 1, No. 2, 501–505, 2007.
  28. Naser-Moghadasi, M., A. Dadgarpour, F. Jolani, and B. S. Virdee, “Ultra wideband patch antenna with a novel folded-patch technique,” *IET Microw. Antennas Propag.*, Vol. 3, No. 1, 164–170, 2009.
  29. Herscovici, N., “New considerations in the design of microstrip antennas,” *IEEE Trans. Antennas Propag.*, Vol. 46, No. 6, 807–811, Jun. 1998.
  30. Low, X. N., Z. N. Chen, and W. K. Toh, “Ultrawideband suspended plate antenna with enhanced impedance and radiation performance,” *IEEE Trans. Antennas Propag.*, Vol. 56, No. 8, 2490–2495, Aug. 2008.